A short duration of chondrule formation in the solar nebula: Evidence from ^{26}Al in Semarkona ferromagnesian chondrules

NORIKO T. KITA,[1],* HIROKO NAGAHARA,[2] SHIGEKO TOGASHI,[1] and YUICHI MORISHITA[1]

[1]Geological Survey of Japan, 1-1-3 Higashi, Tsukuba 305-8567, Japan
[2]Department of Earth and Planetary Science, University of Tokyo, Hongo, Tokyo 113-0033, Japan

Abstract—The ^{26}Al–^{26}Mg systems of five ferromagnesian chondrules from the least metamorphosed ordinary chondrite Semarkona (LL3.0) were studied using a secondary ion mass spectrometer. Their glass or plagioclase portions contain excesses of ^{26}Mg, and in two chondrules the ^{26}Mg excesses are well correlated with ^{27}Al/^{24}Mg, which demonstrates the in-situ decay of ^{26}Al. The initial ^{26}Al/^{27}Al ratios in these chondrules obtained from the slope of isochrons show a narrow range of between 6×10^{-6} and 9×10^{-6}, indicating their short formation duration of less than 1 My. If the solar nebula was initially homogeneous in Al isotopes, the chondrule formation ages are ~2 My younger than those of CAIs. Our results based on the study of the least metamorphosed UOC are consistent with the previous studies on Al-rich chondrules that the chondrule formation started at least 2 My after CAIs. Alternatively, the older records before 2 My were erased by chondrule recycling process. It further suggests that the young apparent ages (3 to >5 My after CAIs) for chondrules in type 3.4 UOCs are due to the disturbance of the ^{26}Al–^{26}Mg system, possibly during parent body metamorphism. The result is not consistent with the extended nebular time scale of >5 My and the chondrule formation by planetary processes. The Ni isotopic analysis of the FeO-rich olivines in a type II chondrule in Semarkona did not show any detectable excess ^{60}Ni in spite of their high Fe/Ni ratios. The upper limit of the initial ^{60}Fe/^{56}Fe ratio of the solar system was estimated to be 3.4×10^{-7}, which is consistent with the previous estimate (0.2–1.9×10^{-7}) from eucrites. This result confirms that the ^{60}Ni excess previously observed from CAIs was not due to the decay of the short-lived nuclide ^{60}Fe, but a Ni isotopic anomaly of nucleosynthetic origin. *Copyright © 2000 Elsevier Science Ltd*

1. INTRODUCTION

The origin of chondrules, particularly the heating mechanism, has been one of the most intensively debated subjects in planetary science since the early 1960s (Wood, 1962). The heating mechanism is related to the thermal evolution of the solar nebula, and thus the determination of the timing of the heating event(s) is crucial to their origin. Despite this importance, the data on the formation age of chondrules is scarce, because of the absence of samples having adequate concentration of elements for precise age determination. Although the ^{26}Al–^{26}Mg system is a useful tool, low abundance of Al and high abundance of Mg in common ferromagnesian chondrules hamper age determinations. Exceptions are Al-rich chondrules (Hutcheon and Jones, 1995; Russell et al., 1996; 1997) and an igneous clast chondrule (Hutcheon and Hutchison, 1989), which make up only less than 1% of all chondrules. Therefore, age determination of common chondrules is expected to give us important information.

We have started a systematic search for excess ^{26}Mg in common chondrules from Semarkona (LL3.0). Unequilibrated ordinary chondrites (UOCs) are divided into subtypes from 3.0 to 3.9 based on the thermoluminescence sensitivity (Sears et al., 1980), which can be used as an index of the effect of thermal metamorphism. Semarkona is classified as 3.0, the least equilibrated ordinary chondrite, while previous chondrule data are mostly obtained from subtype 3.4 UOCs or higher petrologic

types (Hutcheon et al., 1994; Hutcheon and Jones, 1995; Russell et al., 1996; 1997). The maximum heating temperature in the parent body is estimated to be less than 260°C for Semarkona (Alexander et al., 1989), while it is as high as 400°C for subtype 3.4 UOCs (Sears et al., 1991). The evidence of aqueous alteration was found in Semarkona from the matrix phases (Alexander et al., 1989) and from radial pyroxene and cryptocrystalline chondrules (Grossman et al., 2000). However, the effect of aqueous alteration appears to be scarce and they are regarded to be primary (Jones, 1996a). For this reason, Semarkona is the most likely meteorite in which chondrules may preserve the undisturbed ^{26}Al–^{26}Mg system since their formation in the solar nebula.

The second purpose of this work is to apply the ^{60}Fe–^{60}Ni system to chondrule chronology. Iron is a major cation in mafic silicate minerals in chondrules with high Fe/Ni ratios, so that the ^{60}Fe–^{60}Ni system can be applied to a majority of chondrules. The existence of live ^{60}Fe (half-life of 1.5 My) in the early solar system was confirmed from the analyses of three eucrites (Shukolyukov and Lugmair, 1993a; 1993b). The initial ^{60}Fe/^{56}Fe ratio of the solar system was estimated to be $(1.6 \pm 0.5) \times 10^{-6}$ from the ^{60}Ni excess found in CAIs (Birck and Lugmair, 1988). This estimate agrees with the ^{60}Fe production by type II super nova which might have triggered the formation of the solar system (Wasserburg et al., 1998). However, this estimation was not obtained on the basis of a ^{60}Fe–^{60}Ni isochron plot, but from a model calculation using the ^{60}Ni excess and Ni content that were measured in the CAI sample and a typical Fe concentration in coarse grained CAIs. Shukolyukov and Lugmair (1993a) suggested that the ^{60}Ni excess observed

* Author to whom correspondence should be addressed (noriko@gsj.go.jp).

in CAIs could be the isotopic anomaly from the nucleosynthetic origin. Using the ^{60}Ni excesses in bulk eucrites, the initial ^{60}Fe/^{56}Fe ratio of the solar system was estimated to be (0.2–1.9) $\times$ 10^{-7} (Shukolyukov and Lugmair, 1996), which is much lower than the result from CAI analyses. Fe-bearing minerals are rare in CAIs and many of them are of secondary origin (e.g., Fuchs, 1971; Wark and Lovering, 1977; Allen et al., 1978). Therefore, the accurate ^{60}Fe/^{56}Fe ratio at the time of CAI formation is very difficult to obtain from the analyses of the ^{60}Fe–^{60}Ni system in CAIs. Our goal is to detect ^{60}Ni excess from ferromagnesian chondrules in Semarkona in order to estimate the ^{60}Fe/^{56}Fe ratio in the early solar system.

2. ANALYTICAL PROCEDURES

2.1. Electron Microprobe Analyses

We have examined the textures and chemical compositions of olivine, pyroxene, plagioclase and glass in more than 40 chondrules in a polished thin section of Semarkona (USNM 1805-9) using a SEM-EDX (JEOL JSM-6400 SEM with Philips PV9900 EDS). Quantitative analyses of major elements in minerals and glasses were performed using an electron microprobe (JEOL JXA-8800R Superprobe) at accelerating voltage of 15 keV with a beam diameter of 2 μm and a beam current of 12 nA for minerals and 3 nA for glasses. The counting time was 20 s for both mineral and glass analyses. Data were reduced with the Bence and Albee correction method.

2.2. SIMS Analyses

The Mg and Ni isotopic analysis was performed using a secondary ion mass spectrometer (SIMS) Cameca IMS-1270 at the Geological Survey of Japan (GSJ). The primary ion of O$_2^-$ was used with an accelerating voltage of 23 kV (-13 kV at the ion source and $+10$ kV at the sample). We did not use O$^-$ primary ion that is commonly used for SIMS Mg and Ni isotopic analyses, because we found that the secondary ionization efficiency of both Mg and Ni increased twice as much by using O$_2^-$ primary ion than O$^-$ primary ion. Compared to O$^-$ ion, sputtering rate for O$_2^-$ ion increases by the factor of $\sqrt{2}$, while secondary ion intensity increases by the factor of 3 for Mg and factor of 4 for Ni. As a result, O$_2^-$ primary ions produce more Mg and Ni secondary ions by the factor of 2 and 3 for Mg and Ni, respectively, from a unit volume of samples. For both Mg and Ni isotopic analyses, the ion image of the sample surface was transferred 200 times to the field aperture plane that locates before the electric static analyzer. In this condition, the width of the secondary ions at the entrance slit plane is ~100 μm, comparable to the entrance slit widths of 90 μm and 75 μm for the analytical conditions with mass resolution power of 3500 and 4500, respectively. As a result, the transmission of the secondary ions was more than 70% in the present study.

2.2.1. Mg isotopic analyses of plagioclase and glass

In order to analyze small areas in mesostasis in chondrules, the size of primary ion spot was set between 3 and 10 μm, corresponding to ion intensity between 5 and 200 pA. In the early stage of this work, a shaped primary beam with homogeneous ion density was achieved only for 10 μm size, and the smaller beam size was achieved by focusing the primary beam with gausian ion density distribution. Therefore, the flat-bottom sputtered crater on the sample surface was obtained only for 10 μm beam size. At the later stage of this work, we replaced the primary beam aperture from a diameter of 50 μm to a diameter of 20 μm, so that the primary beam size was reduced to approximately 5 μm without losing the homogeneity of the ion density.

The mass resolution was set to 3500 in order to separate MgH$^+$ and Ca^{++} interference from Mg isotopes. In this condition, we could achieve the transmission of secondary ion to be better than 80%, which is similar to the typical condition of the U–Pb dating of zircon for the IMS-1270. The secondary ion intensities of ^{24}Mg and ^{27}Al were 10^3–10^5 cps and 10^5–10^7 cps, respectively, during the analyses of chondrules. Secondary ions were detected by using the electron multiplier

(EM) with pulse-counting mode for intensities less than 3 $\times$ 10^5 cps and Faraday cup for ^{27}Al ions higher than 3 $\times$ 10^5 cps. The EM dead time was estimated in each series of analyses using terrestrial standards by a similar procedure described in Kita et al. (1998). In the analyses made in March and June 1998, the dead time was estimated to be 20 ns for analyses of standards using 10 μm primary beam. However, for the analyses using 5 μm homogeneous primary beam in November, 1998 and January, 1999, the dead time was estimated to be 27 and 37 ns, respectively. In the previous studies on isotopic analyses of various elements in our laboratory, the EM dead time was always nearly 20 ns with a few ns uncertainty (Kita et al., 1998; Morishita et al., 1998). We do not know the reason for this long dead time in the analyses using 5 μm primary ion beam. Because the secondary ion optics of the IMS-1270 is designed to focus sample image on the first dynode of the electron multiplier, there may be a certain effect of exposing intense secondary ions on a limited area on the first dynode. Nevertheless, the effect of dead time variation is negligibly small for most analyses in chondrules with 5 μm beam size because of low ^{24}Mg ion intensities (maximum 0.2‰ shift for 10^4 cps count rate). The measured ^{26}Mg/^{24}Mg ratios were corrected for mass fractionation using the measured ^{25}Mg/^{24}Mg ratios by the following equation:

$$(^{26}Mg/^{24}Mg)_c = (^{26}Mg/^{24}Mg)_m/((^{25}Mg/^{24}Mg)_m/(^{25}Mg/^{24}Mg)_{ref})^2, \quad (1)$$

where $(^{25}Mg/^{24}Mg)_{ref}$ is the normalized value of 0.12663 from Catanzaro et al. (1966). The measured $(^{25}Mg/^{24}Mg)$ ratios in both standards and samples do not fractionate more than 1% from the normalization value, so that choice of fractionation law does not cause any significant difference for the corrected $(^{26}Mg/^{24}Mg)$ ratios. The mean value of the normalized ^{26}Mg/^{24}Mg ratios for terrestrial standards obtained by using a single Faraday Cup detector was 0.139 328 $\pm$ 0.000039, which is in agreement with the literature data (Catanzaro et al., 1966). The repeated analyses of glass and plagioclase standards using EM detector (both 10 μm and 5 μm beam analyses; Table 2) well agree with the value obtained from Faraday cup detector.

Relative sensitivity factor of (^{27}Al/^{24}Mg) was estimated for terrestrial glass and plagioclase standards. The relative sensitivity factors among geological glass standards (Stoll and Jochum, 1999) with various chemical compositions (basalt, andesite, ryolite) agree within 5%, and those between An95 and An60 plagioclase standards agree within 10% (Mostefaoui, unpublished data). Therefore, for all the glass and plagioclase data in chondrules, the (^{27}Al/^{24}Mg) ratios were corrected using the sensitivity factors of basalt glass standard (fused glass from JB1a geological standard) and average plagioclase standards (An95 and An60) analyses, respectively, with applying 10% error for the correction. The sensitivity factor for more Na-rich plagioclase ($\leq$An 30) is assumed to be 20% because we do not measure plagioclase standards with higher albite compositions.

In many cases, sputtering Ca-pyroxene microcrystallites in the mesostasis caused high Mg ion intensity and low Al/Mg ratio. Therefore, it was necessary to avoid sputtering of Ca-pyroxene during analyses. We applied two different methods to locate primary ion beam to the area with high Al/Mg ratio. In the earlier series of analyses, a direct ion image was obtained using the ion-microscope mode before each analysis in order to select the best position with a high Al/Mg ratio. The mesostasis area was sputtered with 10 μm primary ion beam and the shapes of the Ca-pyroxene microcrystallites in a mesostasis were observed with spatial resolution of 1 μm in the ^{24}Mg and ^{27}Al secondary ion images. The primary ion beam was then focused to 3 μm or 5 μm to sputter the narrow area to get a high ^{27}Al/^{24}Mg secondary ion intensity ratio for the isotopic analysis. In the later series of analyses with 5 μm homogeneous primary beam, we sputtered several positions of the sample near the high Al/Mg region for a short time and observed ^{27}Al and ^{24}Mg ion intensities. The automated program was used for analyzing many positions by moving the sample stage every 10–15 μm. Spots with high ^{27}Al/^{24}Mg ratio were then selected and examined by the direct ion imaging before isotopic analyses, in order to confirm the absence of tiny high-Mg phases in the observed area. The removal of C-coating was minimized in the latter method, which has an advantage of avoiding any surface charging problems and reducing the ionization of Mg from surrounding Mg-rich phases.

2.2.2. Mg isotopic analyses of olivines and pyroxenes

The Mg isotopic ratios of Mg-rich phases were measured with multi-collection system using three Faraday cups, which was lately equipped with IMS-1270 at GSJ. The three isotopes of Mg were detected simultaneously using three faraday cups with resisters of 10^{10} Ω for ^{24}Mg and $10^{11}\Omega$ for ^{25}Mg and ^{26}Mg. Faraday cup background was measured before and after each measurement. The primary ion beam size was 10 μm with 0.2–0.4 nA intensity. The Mg secondary ion intensity was between 3×10^7 and 6×10^7 cps. The mean value of $(^{26}Mg/^{24}Mg)_c$ ratios of terrestrial olivine standards was slightly deviated from the literature value ($\sim$0.5‰) with the reproducibility of 0.2‰. Although amplifiers of multicollectors are calibrated using the reference current in the revel of 10^{-4}, there is a small but detectable discrimination for the measured isotopic ratios. Therefore, all the multicollector results were corrected for this discrimination by assuming that the mean value of $(^{26}Mg/^{24}Mg)_c$ of terrestrial standards is the same as the literature value.

2.2.3. [60]Fe–[60]Ni analyses

The Ni isotopic analyses were performed for CH4, which has large FeO-rich olivine phenocrysts. The details of the analytical conditions and calibration for matrix effects are described in Kita et al. (1998). In order to separate molecular interference of CaO, and Si$_2$, mass resolution was set to 4500. The tailing of Ni and Fe hydrides was much less than 0.1‰ at the center of the Ni isotope mass spectrums. In this work, analytical conditions were modified as follows: (1) The O_2^- primary ion was used instead of O^- ion for better ionization efficiency. (2) The diameter of the primary ion was reduced to 15 μm with intensity between 0.5 and 1.5 nA. (3) The width of secondary ion at the entrance slit plane was reduced from $\sim$200 μm to $\sim$100 μm by changing the magnification of the ion image between sample surface to field aperture plane from 100 times to 200 times. As a result, we improved the total transmission from 25% to 70% and the ionization efficiency 5 times higher than before. The typical secondary ^{60}Ni ion intensity for CH4 olivine with 50 ppm Ni content was 2×10^3 cps/nA. The measured $(^{60}Ni/^{61}Ni)$ ratios were corrected for dead time of the detector and the instrumental mass fractionation by applying normalization to the literature value of $(^{60}Ni/^{61}Ni) = 3.1760$ (Birck and Lugmair, 1988). The permil deviation of corrected $(^{60}Ni/^{61}Ni)$ from the literature value of 23.100 (Birck and Lugmair, 1988) is expressed as $\delta(^{60}Ni)$. The mean value of $\delta(^{60}Ni)$ of 15 analyses of terrestrial olivine standard was -0.12 ± 0.29‰. The measured Fe/Ni ratios were corrected for SIMS relative sensitivity factor between Fe and Ni which is obtained from terrestrial olivine standards (Fo89, Fo70, and Fo60) with known Ni concentrations (Kita et al., 1998).

3. RESULTS AND DISCUSSION

3.1. Sample Descriptions

Most of these chondrules in the Semarkona thin section were common ferromagnesian chondrules that show typical porphyritic texture and composed of olivine and pyroxene grains with approximately chondritic bulk chemical compositions. They are usually classified into FeO-poor (or Mg-rich; type I) and FeO-rich (type II) groups based on the molar FeO/(MgO + FeO) ratios of olivine and pyroxene; 0–10% for type I and >10% for type II (Scott and Taylor, 1983). In the previous ^{26}Al–^{26}Mg studies on chondrules (Hutcheon and Jones, 1995; Russell et al., 1996; 1997), calcic plagioclase in Al-rich chondrules was the major target to detect ^{26}Mg excess. Ferromagnesian chondrule glasses usually contain significant amount of MgO (1–10 wt.%), so that their Al/Mg ratios are usually less than 10 in spite of their high Al$_2$O$_3$ contents (10–30 wt.%). Some porphyritic chondrules contain abundant Ca-pyroxene in the mesostasis as microcrystallites and the surrounding glasses are enriched in Al$_2$O$_3$ (10–20%) and depleted in MgO (<1%)

so that the Al/Mg ratios are as high as 50 to 200. Many of them show a complex structure of microcrystallites in the scale of less than a few μm, which are too fine to be avoided in the SIMS analysis with 3–5 μm spot. We selected two chondrules that contain Ca-pyroxene free glass area larger than SIMS spot ($\geq$10 μm) for the Al–Mg study. Three other chondrules having interstitial plagioclase (10–20 μm) were also selected for the Al–Mg study. A list of analyzed chondrules with their representative mineral compositions is given in Table 1. Chondrules CH4 and CH36 are FeO-rich porphyritic olivine–pyroxene chondrules (type II), CH3 is a FeO-poor porphyritic olivine–pyroxene chondrule (type I), CH23 is a FeO-rich nonporphyritic olivine–pyroxene chondrule (type III), and CH60 is a fragment of a FeO-rich porphyritic pyroxene chondrule (type II). Back scattered electron images of these chondrules are shown in Fig. 1. The contents of plagioclase and/or glass in these chondrules are 5–15%, so that their Al$_2$O$_3$ contents are less than 5%. Therefore, these chondrules are not Al-rich chondrules, but common ferromagnesian chondrules.

CH4 and CH36 are similar to typical type II chondrules that were described by Jones (1990; 1996a). They contain glassy mesostasis with abundant Ca–pyroxene microcrystallites. Olivine phenocrysts in CH4 are large ($\sim$100 μm) and show normal zoning in the core (Fo = 88–83) with higher FeO contents at the rim (Fo = 75). Low Ca pyroxene phenocrysts are smaller than olivine and zoned (En = 77–83, Ws = 1–5). CH36 is rich in pyroxene with complex zoning (En = 75–80). In glassy mesostasis, some areas are free from Ca–pyroxene microcrystallites in a scale of larger than 10 μm. Chemical compositions of these areas are rich in SiO$_2$, Al$_2$O$_3$, and Na$_2$O (66–70% SiO$_2$, 17–20% Al$_2$O$_3$, and 2–8% Na$_2$O) and depleted in CaO (<2%) and MgO (<0.5%). The SIMS Al–Mg analyses were done for these areas which show high Al/Mg ratios (>50). An example of the analyzed area in chondrule mesostasis is shown in Fig. 2.

A type I chondrule CH3 is slightly different from typical type I chondrules described by Jones and Scott (1989) and Jones (1994). The low Ca pyroxene phenocrysts have magnesian cores [molar MgO/(FeO + MgO) $\sim$ 0.97] and are surrounded by low Ca and high Al pyroxene (Al$_2$O$_3$ $\sim$10%). The mesostasis consists of anhedral Ca pyroxene with high Al$_2$O$_3$ contents (8–17%) and plagioclase that is nearly pure anorthite. Plagioclase contains a significant amount of fine grained inclusions of possible Ca pyroxene.

In a nonporphyritic chondrule CH23, coarse olivine and low Ca-pyroxene grains are FeO-rich and show weak zoning (Fo = 81–83, En = 83–76 Wo = 2–5). Nearly pure anorthite and minor Ca–pyroxene (Wo = 16–35) occur as interstitial phases. Because of its nonporphyritic texture and low alkali contents, CH23 appears to be similar to a noritic clast chondrule 1805-5 CC1 in Semarkona studied by Hutcheon and Hutchison (1989). Although they discussed the origin of CC1 as an igneous rock derived from a differentiated planetary body, its bulk chemical composition is chondritic (Hutcheon and Hutchison, 1989). This sample can be a chondrule without common texture. Therefore, hereafter we assume that both CH23 and CC1 are minor types of ferromagnesian chondrules, but not a fragment of igneous rocks formed in a differentiated parent body.

The chondrule CH60 may be a fragment of type II pyroxene chondrule, but it is not similar to typical type II chondrules

Table 1. Selected EPMA analyses (wt.%) of minerals in chondrules from Semarkona (LL3.0).

Sample/mineral	SiO_2	TiO_2	Al_2O_3	Cr_2O_3	FeO	MnO	MgO	CaO	Na_2O	K_2O	Total	Composition[a]
CH4 (Type II POP)												
Olivine	38.59	0.01	0.01	0.51	15.23	0.40	45.40	0.09	0.02	0.00	100.26	Fo84
Olivine	38.06	0.00	0.00	0.63	18.77	0.53	42.01	0.15	0.04	0.01	100.21	Fo80
Pyroxene	54.39	0.05	0.27	0.98	12.97	0.58	30.05	0.95	0.03	0.00	100.27	Wo2 En79 Fs19
Glass	68.90	0.19	19.48	0.03	1.08	0.04	0.22	0.43	8.46	0.37	99.22	
CH36 (Type II POP)												
Olivine	37.60	0.00	0.01	0.50	21.92	0.59	38.85	0.11	0.02	0.00	99.61	Fo76
Pyroxene	54.22	0.03	0.28	0.90	15.47	0.64	27.67	0.94	0.06	0.00	100.21	Wo2 En75 Fs23
Ca-pyroxene	50.95	0.29	1.21	1.68	13.87	0.68	13.62	15.56	0.56	0.02	98.45	Wo34 En42 Fs24
Glass	66.47	0.49	17.53	0.01	6.23	0.15	0.34	0.84	2.37	0.96	95.37	
CH3 (Type I POP)												
Olivine	40.95	0.00	0.02	0.41	3.40	0.07	55.17	0.15	0.00	0.00	100.17	Fo97
Pyroxene	56.41	0.22	2.10	0.69	2.14	0.02	36.28	1.79	0.01	0.00	99.67	Wo3 En94 Fs3
Al-pyroxene	51.38	0.60	9.10	0.72	2.72	0.06	32.36	2.94	0.01	0.00	99.89	Wo6 En90 Fs4
Ca-pyroxene	46.75	1.10	12.53	0.90	1.33	0.08	15.53	21.98	0.01	0.01	100.20	Wo34 En48 Fs2 Tsch15
Plagioclase	44.00	0.00	34.45	0.02	0.33	0.03	0.55	19.43	0.03	0.00	98.84	An99.7
CH23 (Type III)												
Olivine	38.66	0.06	0.05	0.62	16.46	0.33	43.17	0.20	0.02	0.00	99.49	Fo82
Pyroxene	54.96	0.06	0.97	1.04	10.59	0.24	30.90	1.15	0.00	0.00	99.90	Wo2 En82 Fs16
Pyroxene	52.74	0.45	3.31	1.44	11.98	0.38	27.48	2.65	0.00	0.00	100.44	Wo5 En76 Fs19
Ca-pyroxene	50.55	0.83	3.52	1.30	7.77	0.33	17.79	16.95	0.01	0.01	99.06	Wo35 En52 Fs13
Plagioclase	46.22	0.05	32.18	0.05	0.71	0.04	0.89	19.14	0.00	0.02	99.29	An 99.9
CH60 (Type II PP)[b]												
Olivine	38.78	0.02	0.00	0.55	13.94	0.74	45.65	0.17	0.01	0.00	99.85	Fo85
Pyroxene	55.59	0.00	0.17	0.65	7.99	0.46	34.39	0.15	0.02	0.00	99.43	Wo0 En88 Fs12
Pyroxene	55.06	0.12	0.87	1.10	9.45	0.85	31.19	1.23	0.01	0.01	99.88	Wo2 En84 Fs14
Pyroxene	54.98	0.10	0.94	1.14	9.84	0.93	30.08	2.61	0.04	0.00	100.65	Wo5 En80 Fs15
Plagioclase	58.85	0.09	24.02	0.00	0.68	0.03	0.19	7.08	7.49	0.20	98.63	An34 Ab65 Or1

[a] Composition of minerals are expressed as Fo (Mg_2SiO_4) for olivine, Wo ($CaSiO_3$), En ($MgSiO_3$), Fs ($FeSiO_3$), and Tsch($Ca_{0.5}AlSi_{0.5}O_3$) for pyroxene, and An($CaAl_2Si_2O_8$), Ab($NaAlSi_3O_8$), and Or($KAlSi_3O_8$) for plagioclase.
[b] Chondrule CH60 is a fragmented chondrule.

described by Jones (1996a). Pyroxene phenocrysts are zoned (0–8 Wo, 88–74 En, and 12–17 Fs) and sometime contain smaller grains of olivine (Fo ∼ 85). The interstitial phase contains albitic plagioclase (An28–An34), minor SiO_2-rich glass, metal–sulfide nodule, and fine grained Ca pyroxene included in plagioclase. The chemical composition of SiO_2-rich glass is very similar to glassy mesostasis in CH4.

Electron microprobe analyses of the chondrule glasses generally have oxide sums close to 100%, suggesting they do not contain significant amounts of hydrous phases that might be derived from aqueous alteration. Therefore, the secondary effect due to the aqueous alteration is most likely did not play a significant roll and, thus, we will not further discuss it.

3.2. The Al–Mg System of Semarkona Chondrules

The results of the isotope analyses are presented in Table 2, and the ^{26}Al–^{26}Mg isochron diagrams are shown in Fig. 3. Most of the analyzed areas have the $^{27}Al/^{24}Mg$ ratios between 50 and 200. All the chondrules show clear excess of ^{26}Mg up to 12‰. Because of low primary intensities with a 3 μm beam size, the low secondary Mg ion intensities resulted in relatively large errors. However, a 5 μm beam size was not always small enough to avoid Ca-pyroxene microcrystallites in the mesostasis of CH4 and CH36 (type II chondrules), so the 3 μm beam size was used in these cases. For CH23, a 10 μm beam size was applied to the plagioclase grains because of the large grain size. For many of the analyzed areas in this sample, the $^{27}Al/^{24}Mg$ ratios decreased during the analysis because tiny inclusions

containing high Mg contents surfaced as the samples were sputtered deeper. For this reason, only a single measurement with a relatively high $^{27}Al/^{24}Mg$ ratio was available for this sample. Mg isotopic compositions of olivine and pyroxene were normal within an error of 0.2‰. The measured $^{25}Mg/^{24}Mg$ ratios in chondrules did not differ more than 1% from the literature value (0.12663) and agree within 5‰ from each terrestrial standard samples (i.e., olivine, glass, and plagioclase standards).

For CH4 and CH36, several data points with various $^{27}Al/^{24}Mg$ ratios were obtained and these data show a linear correlation between the $^{27}Al/^{24}Mg$ and $^{26}Mg/^{24}Mg$ ratios (Fig. 3A,B). This is the first clear evidence for the former presence of live-^{26}Al at the time of formation of FeO-rich porphyritic (type II) chondrules. The initial $^{26}Al/^{27}Al$ ratio at the time of formation of each chondrule, here after denoted as $(^{26}Al/^{27}Al)_0$, was estimated from the slope of the isochron by the least square fitting of the data. These results fall in a narrow range between 6×10^{-6} and 9×10^{-6}. There is no significant difference among chondrules with different FeO contents of olivine and pyroxene and alkali contents of mesostasis.

Assuming that the ^{26}Al was homogeneously distributed in the early solar system, the small differences among the estimated $^{26}Al/^{27}Al$ ratios of chondrules reflect small variations in their formation time. The reference time ($t = 0$) is chosen to be the time of CAI formation with the $^{26}Al/^{27}Al$ ratio of 4.5×10^{-5} (from the peak value of type B1 CAIs; MacPherson et al., 1995). The formation ages of five chondrules relative to CAIs
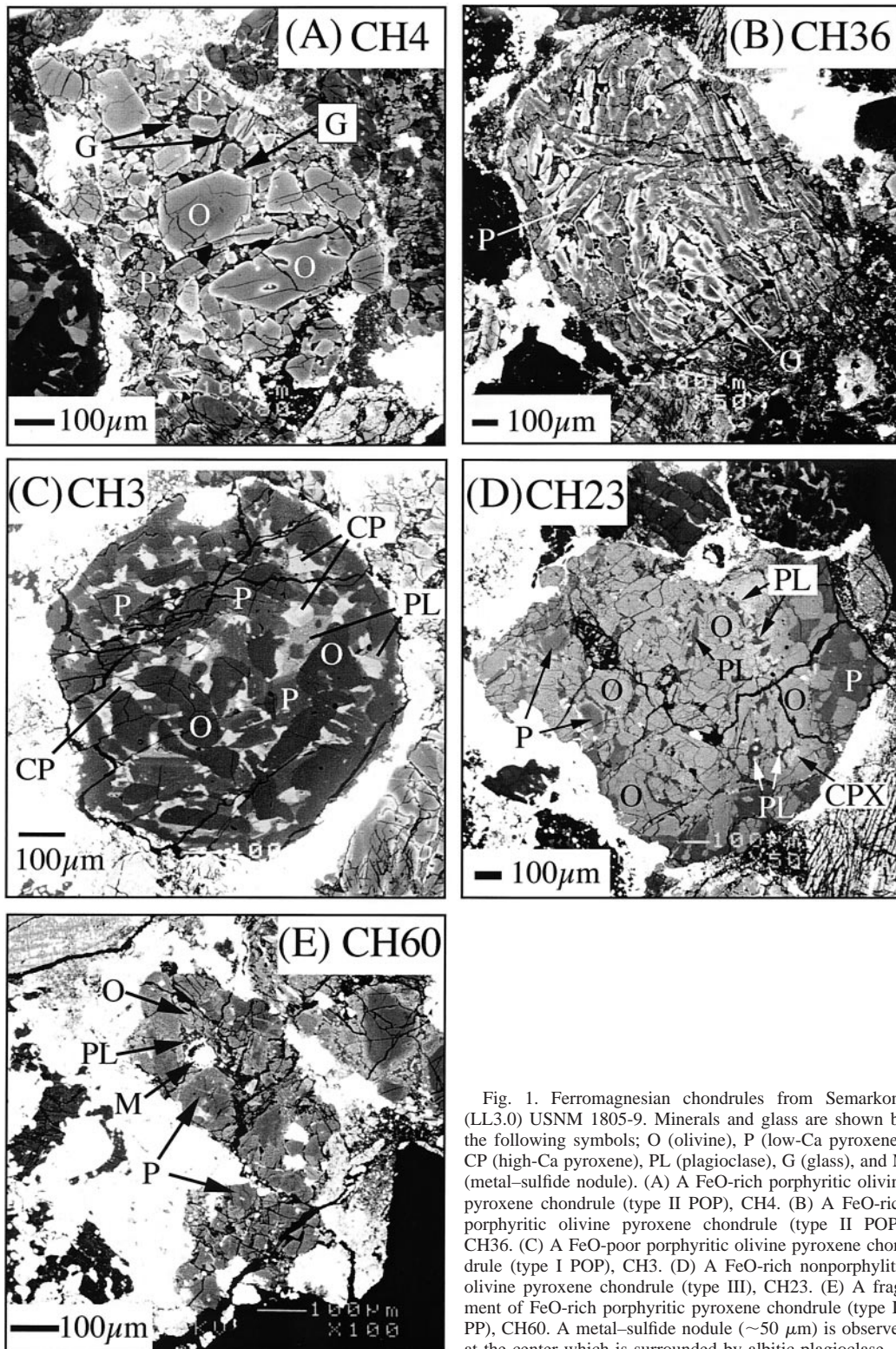
Fig. 1. Ferromagnesian chondrules from Semarkona (LL3.0) USNM 1805-9. Minerals and glass are shown by the following symbols; O (olivine), P (low-Ca pyroxene), CP (high-Ca pyroxene), PL (plagioclase), G (glass), and M (metal–sulfide nodule). (A) A FeO-rich porphyritic olivine pyroxene chondrule (type II POP), CH4. (B) A FeO-rich porphyritic olivine pyroxene chondrule (type II POP), CH36. (C) A FeO-poor porphyritic olivine pyroxene chondrule (type I POP), CH3. (D) A FeO-rich nonporphyritic olivine pyroxene chondrule (type III), CH23. (E) A fragment of FeO-rich porphyritic pyroxene chondrule (type II, PP), CH60. A metal–sulfide nodule (~50 μm) is observed at the center which is surrounded by albitic plagioclase.
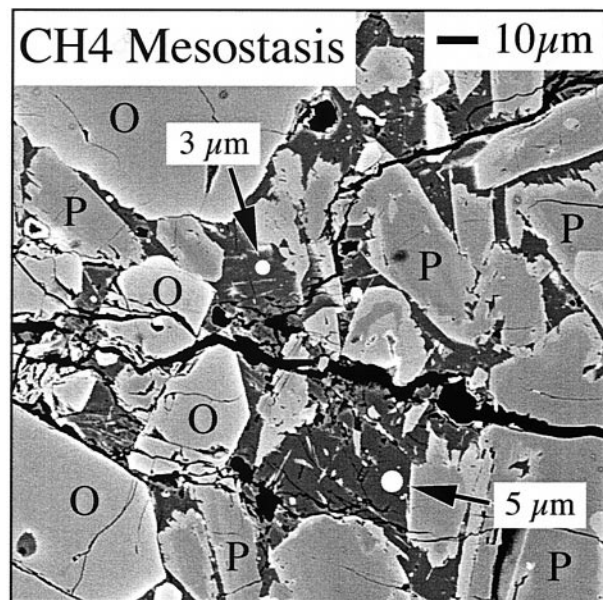
Fig. 2. A mesostasis area of CH4. Olivine and pyroxene phenocrysts are set in glassy mesostasis. Fine Ca-pyroxene microcrystallites are scattered in the glass, which are seen as bright fine fibers in dark glass. The examples of SIMS spot sizes (3 and 5 μm diameters) are shown as white dots, which avoids sputtering Ca-pyroxene microcrystallites.

Table 2. Results of Mg isotopic analyses of Semarkona chondrules.[a]

Sample[b]	Phase	Beam size	$^{27}Al/^{24}Mg$[c]	$(^{26}Mg/^{24}Mg)_c$[d]
Chondrules				
CH4				
−1	Glass	3 μm	99	0.14083 ± 0.00098
−2	Glass	3 μm	41	0.13936 ± 0.00097
−3-1	Glass	5 μm	208	0.14125 ± 0.00054
−3-2	Glass	5 μm	181	0.14112 ± 0.00057
−3-3	Glass	5 μm	139	0.14038 ± 0.00047
−3-4	Glass	5 μm	123	0.14033 ± 0.00044
−4	Olivine	10 μm	=0	0.139330 ± 0.000026
CH36				
−1	Glass	3 μm	44	0.13966 ± 0.00058
−2	Glass	3 μm	115	0.14070 ± 0.00110
−3	Glass	5 μm	45	0.13948 ± 0.00027
−4	Glass	5 μm	48	0.13978 ± 0.00031
−5	Glass	5 μm	96	0.14012 ± 0.00040
−6	Glass	5 μm	282	0.14101 ± 0.00068
−7	Olivine	10 μm	=0	0.139340 ± 0.000026
CH3				
−1	An100	5 μm	67	0.14016 ± 0.00049
−2	An100	5 μm	81	0.13985 ± 0.00046
−3	An100	5 μm	61	0.13992 ± 0.00034
−4	An100	5 μm	59	0.13968 ± 0.00034
−5	Olivine	10 μm	=0	0.139291 ± 0.000054
CH23				
−1	An100	10 μm	39	0.13969 ± 0.00020
−2	Olivine	10 μm	=0	0.139328 ± 0.000026
CH60				
−1	An30	5 μm	152	0.14012 ± 0.00048
−2	An30	5 μm	85	0.13990 ± 0.00036
−3	Pyroxene	10 μm	=0	0.139335 ± 0.000026

Average of standards	
FC single	0.139328 ± 0.000039
EM 1998 June	0.139354 ± 0.000060
EM 1998 Nov.	0.139359 ± 0.000044
EM 1999 Jan.	0.139312 ± 0.000058
FC multi[5] 1999 May	0.139417 ± 0.000054
FC multi[e] 2000 Feb.	0.139384 ± 0.000026

[a] Errors equated with data are 2σ error (95% confidence).
[b] The numbers after chondrule names indicate individual SIMS spot numbers. The third spot from CH4 was measured four times with increasing depth.
[c] The analytical errors of ($^{27}Al/^{24}Mg$) ratios were 10% for glass and anorthosite, and 20% for plagioclase with more albitic composition.
[d] Data are corrected for mass fractionation during the SIMS analyses.
[e] A small amount of discrimination was observed for the multicollector data compared to both the literature (0.139 32) and FC single collector. Olivine and pyroxene data were corrected for this discrimination.

are calculated to be nearly 2 My young, between 1.7 and 2.2 My (Fig. 3). Therefore, the Semarkona ferromagnesian chondrules formed over a narrow time range of less than 1 My.

3.3. The Variation of the Initial $^{26}Al/^{27}Al$ Among UOC Chondrules

Our results are compared in Fig. 4 to the data for individual chondrules from Semarkona (Hutcheon and Hutchison, 1989) and the other unequilibrated ordinary chondrites (Russell et al., 1996; 1997). The clast chondrule from Semarkona 1805-5 CC1 (Hutcheon and Hutchison, 1989) shows an initial $^{26}Al/^{27}Al$ ratio of 7.7 × 10^{-6} which is very close to our results. Therefore, ferromagnesian chondrules in Semarkona including 1805-5 CC1 show similar $^{26}Al/^{27}Al$ ratios, but their chemical compositions, mineralogy, and texture vary. The molar FeO/(MgO + FeO)% of olivine and pyroxenes vary from 3 to 25%, and the interstitial phases include Al_2O_3, Na_2O, SiO_2-rich glass and plagioclase either nearly pure anorthitic or more albitic composition. Such variations indicate that these chondrules were derived from different precursor materials and experienced different physical conditions during their formation (in terms of heating temperature, volatile loss, oxygen fugacity, and cooling rate). Therefore, it is likely that various types of chondrules formed within a short time.

The initial $^{26}Al/^{27}Al$ ratios of chondrules obtained from the other UOCs (Russell et al., 1996; 1997) are equal to or lower than those of Semarkona. Most of lower initial $^{26}Al/^{27}Al$ ratios were obtained from plagioclase bearing chondrules in Chainpur LL3.4 chondrite. Previous authors interpreted these lower initial $^{26}Al/^{27}Al$ ratios either by younger age of formation or by resetting prior to incorporation in the parent body, but not by the disturbance of ^{26}Al–^{26}Mg system during the thermal meta-

morphism in their parent body (Russell et al., 1996; 1997; LaTourrette and Wasserburg, 1998). Type 3.4 UOC chondrites like Chainpur might be heated up to a temperature of 400°C in their parent body (Sears et al., 1991). The Mg self-diffusion in anorthite crystal at this temperature is too slow to reset the ^{26}Al–^{26}Mg system, as discussed by LaTourrette and Wasserburg (1998). Therefore, the younger chondrule ages of Chainpur Al-rich chondrules cannot be explained by the parent body metamorphism, if the self-diffusion of Mg isotopes between
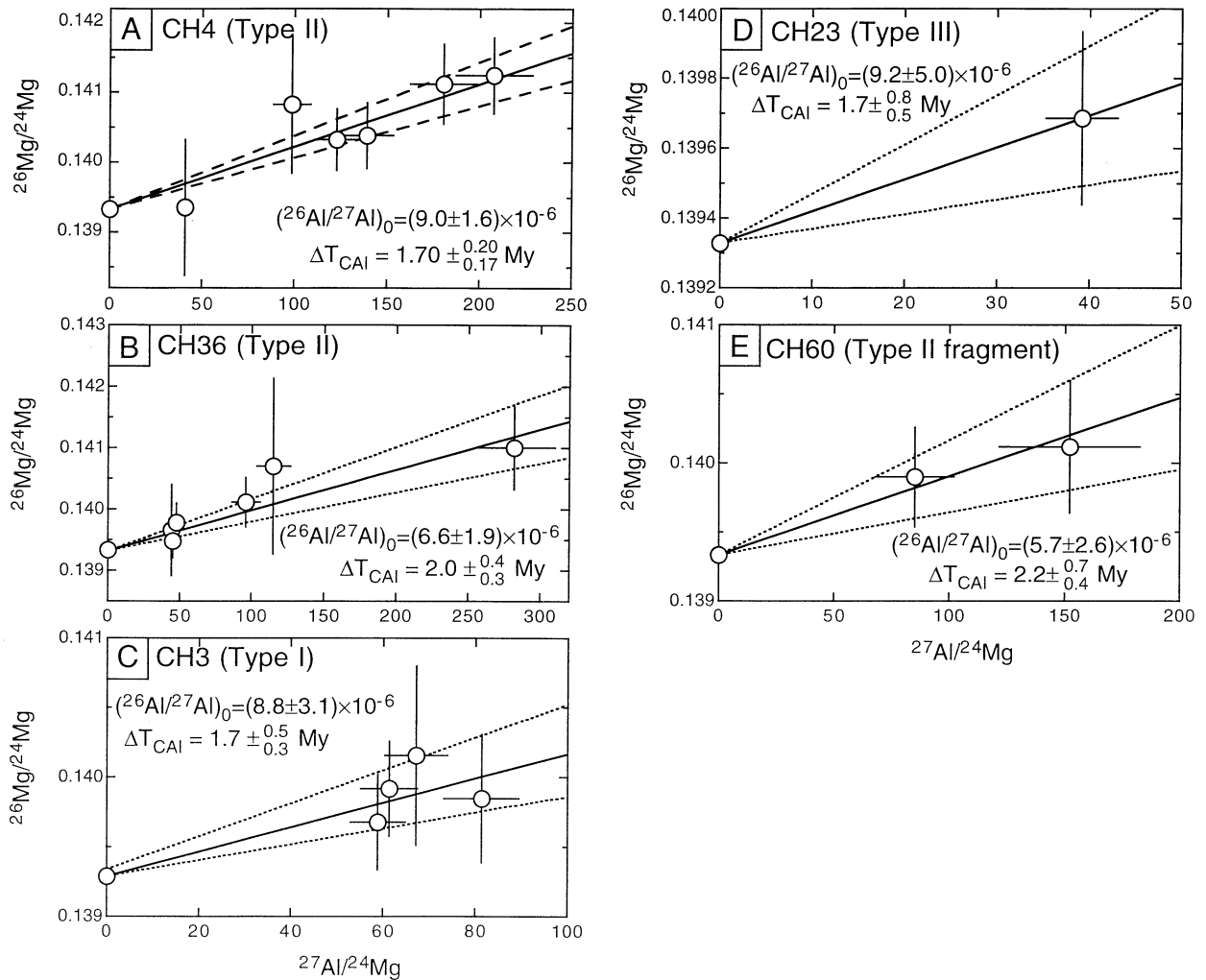
Fig. 3. The ^{26}Al–^{26}Mg isochron plots for individual chondrules from Semarkona (LL3.0). The initial ^{26}Al/^{27}Al isotopic ratio of each chondrule, $(^{26}$Al/^{27}Al$)_0$, was calculated from the slope of the isochron by the least square fitting (using the program made by Ludwig, 1989). The error bars equated to data are 2σ error. The isochron with the corresponding 2σ error limits for its slope are shown as solid and dashed lines, respectively. The relative age after CAI formation is calculated as $\Delta T = \ln\{(^{26}$Al/^{27}Al$)_0/4.5 \times 10^{-5}\}/\ln(2) \times 0.73$ My. (A) CH4, (B) CH36, (C) CH3, (D) CH23, (E) CH60.

anorthite and Mg-bearing minerals is the only process to reset the ^{26}Al–^{26}Mg isotope system.

Our new results of Semarkona chondrules showing systematically higher initial ^{26}Al/^{27}Al than Chainpur chondrules suggest that the thermal metamorphism might affect the ^{26}Al–^{26}Mg system even for type 3.4 chondrites. There are many lines of evidence for the open system behavior of chemical elements in chondrules by the thermal metamorphism of UOC. McCoy et al. (1991) showed that the Fe–Mg exchange process among mafic silicates is evident for subtype 3.3, and only Semarkona preserved the original Fe and Mg distribution before the metamorphism started. They observed that the degree of recrystallization in chondrule mesostasis increases with petrologic subtypes, from rarely recrystallized Semarkona (LL3.0) to mostly recrystallized Parnallee (LL3.6). From the cathodoluminescence study of UOC chondrules, Sears et al. (1992) found that the chemical compositions of chondrule mesostasis have changed from the original composition during the thermal

metamorphism, even between subtypes 3.0 and 3.4. The proportion of chondrules with anorthite- and quartz- normative mesostasis decreases from type 3.0 to 3.4 and the chondrule mesostasis becomes more closed to albitic composition and homogenized for higher petrologic types. Therefore, the ^{26}Al–^{26}Mg system in type 3.4 UOCs chondrules could be disturbed by elemental mobilization of Mg during the metamorphism, such as Mg loss from Si- and Al-rich glass and calcic plagioclase to olivine and pyroxenes. Indeed, the Al-rich chondrules with younger ages show high ^{27}Al/^{24}Mg ratios between 200 and 650, while those in older chondrules are less than 100 (Srinivasan et al., 1996; Russell et al., 1996; 1997). The pyroxene included in glass in Chainpur 1251-16-3 chondrule is reported to show the excess ^{26}Mg in spite of its low ^{27}Al/^{24}Mg (Russell et al., 1997). These data indicate that the loss of Mg from Al-rich phases without homogenizing Mg isotopes, possibly by the chemical diffusion of Mg between Fe and/or Ca that is usually orders of magnitude faster than the self-diffu-
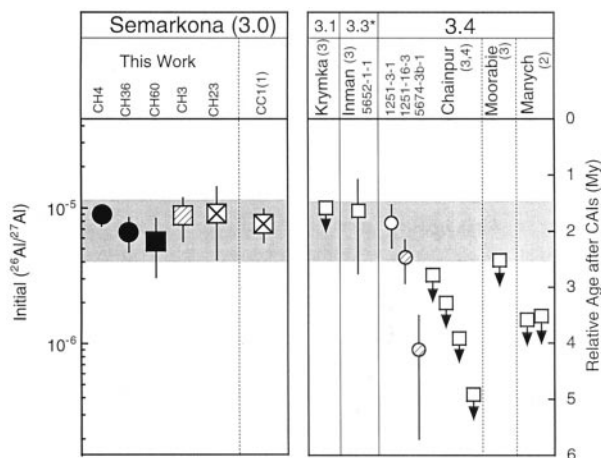
Fig. 4. The initial ^{26}Al/^{27}Al ratios of UOC chondrules and their relative formation ages to the CA1 formation. The data are shown in the order of increasing metamorphic grades of host meteorites. The number in the parentheses after sample names indicate the source of the published data as follows; (1) Hutcheon and Hutchison (1989), (2) Hutcheon and Jones (1995), (3) Russell et al. (1996), and (4) Russell et al. (1997). Inman is a breccia containing both LL3.3 and LL3.6. These meteorites belong to the LL-group UOC, except for Moorabie which belongs to the L-group. Symbols indicate the chondrule chemical composition and the analyzed Al-bearing phases. The Al-rich chondrules are shown by open symbols, type I chondrules by shadowed symbols, type II chondrules by filled symbols, and type III chondrules by crossed symbols. The Al-bearing phase of each chondrule is indicated by squares for plagioclase and by circles for glass. The data presented as the upper limits of the initial ^{26}Al/^{27}Al ratios are shown by symbols with arrows. Semarkona ferromagnesian chondrules indicate the narrow range of the formation time (shown as the shadowed area) compared to the chondrules from type 3.4 UOCs.

sion. Further investigations for type 3.4 UOC chondrules are required to clarify the effect of the thermal metamorphism on the ^{26}Al–^{26}Mg system.

Two Al-rich chondrules with high ^{26}Al/^{27}Al ratios, Inman 5652-1-1 and Chainpur 1251-3-1 (Russell et al., 1996), are a good indicator for formation of Al-rich chondrules contemporary with ferromagnesian chondrules. It should be emphasized that the Al–Mg study of ferromagnesian chondrules in this work strengthened the fact that the initial ^{26}Al/^{27}Al ratios of chondrules are at least five times lower than that of CAIs. It corresponds to the formation age of chondrules ~2 My younger than CAIs if the difference is converted to the time difference.

Recent ^{53}Mn–^{53}Cr studies on the individual Chainpur (LL3.4) and Bishunpur (LL3.1) chondrules indicate the chondrule formation ~6 My after CAIs (Nyquist et al., 1997; 1999), which is comparable to the younger ^{26}Al ages in type 3.4 UOC chondrules. However, the interpretation of the ^{53}Mn–^{53}Cr data needs some considerations. First, if the ^{53}Cr abundance in CAIs is anomalous due to the nucleosynthetic origin (Lugmair and Shukolyukov, 1998), the time difference of ~6 My between chondrules and CAIs is erroneous. Second, the ^{53}Mn–^{53}Cr data were obtained as bulk chondrule isochron that corresponds to the time of the Mn/Cr fractionation among chondrules (or their precursors), while the ^{26}Al–^{26}Mg internal isochron indicates the time of the last melting event or metamorphism for each chondrule. If the bulk Mn/Cr ratios and Cr isotopes in each

chondrule was in a closed system during the thermal metamorphism, the fact that the ^{53}Mn–^{53}Cr data of chondrules lie on the single isochron may indicate their formation in a narrow time scale. Then, it will be consistent with our results of the short duration (<1 My) of chondrule formation.

3.4. The ^{60}Fe–^{60}Ni System in CH4 and the Initial ^{60}Fe Abundance in the Solar System

The Ni contents in CH4 olivines were as low as 45 ppm, resulted in the Fe/Ni ratios as high as 2,400. However, we do not observe any resolvable ^{60}Ni excess. The mean value of all the analyses (20 data) was $\delta(^{60}$Ni$) = -0.05 \pm 0.99$‰. The upper limit of the ^{60}Fe/^{56}Fe at the time of the CH4 formation is estimated to be 1.4×10^{-7} with the mean ^{56}Fe/^{60}Ni ratio of 6,640 in olivines. Using the upper limit of the age of CH4 (1.90 My after CAIs), we obtain the upper limit of ^{60}Fe/^{56}Fe $< 3.4 \times 10^{-7}$ at the time of CAI formation.

This value is significantly lower than the estimate of ^{60}Fe/^{56}Fe $= (1.6 \pm 0.5) \times 10^{-6}$ from an Allende CAI (Birck and Lugmair, 1988), but consistent with the recent estimate of $(0.2–1.9) \times 10^{-7}$ (Shukolyukov and Lugmair, 1996) from eucrites. The apparent ^{60}Ni excess found in CAIs is probably due to an isotopic anomaly of the nucleosynthetic origin, as suggested by Shukolyukov and Lugmair (1993a). If the initial ^{60}Fe/^{56}Fe ratio of the solar system was as low as 6×10^{-8} which is the best estimate of Shukolyukov and Lugmair (1996), the ^{60}Ni excess in CH4 olivine is only 0.2‰, which is too small to be resolved using the present SIMS technique.

The ^{60}Fe abundance in the initial solar system is related to the production of this nuclide in the stellar source. If the formation of the solar system was triggered by the single type II super nova, the ^{60}Fe/^{56}Fe ratio of the initial solar system is estimated to be between 3×10^{-7} and 1×10^{-5} (Wasserburg et al., 1998). Both our present result and the estimate by Shukolyukov and Lugmair (1996) indicate that the initial ^{60}Fe/^{56}Fe ratio of the solar system is much less than that produced by type II super nova and may be consistent with the production from AGB stars (Wasserburg et al., 1994). Therefore, our result does not support the idea of formation of the solar system by the super nova trigger.

3.5. Implication to Chondrule Formation

Here, we assume that the variation of the initial ^{26}Al/^{27}Al ratios in meteoritic samples represent the difference in their formation ages. There are various models for chondrule formation, which are basically divided into three: (1) remelting of dust in the solar nebula, (2) planetary processes, and (3) direct condensation. Although the recent models for liquid condensation (Yoneda and Grossman, 1995; Ebel and Grossman, 2000) indicate the possibility that chondrules could form by condensation in the solar nebula, presence of relict grains (Nagahara, 1981; Jones, 1996b) implies that the chondrules formed by the melting of solid precursors. Russell et al. (1996) suggested an extended nebular time scale of >5 My on the basis that both ^{26}Mg excess bearing and ^{26}Mg excess free chondrules exists in the same chondrite. At the same time, there is increasing evidence that the geological activities on asteroidal sized planetary bodies started as early as 3 My after CAI formation. For

example, thermal metamorphism of the ordinary chondrite parent bodies started at least 3–6 My after CAIs (Zinner and Göpel, 1992; Göpel et al., 1994). The ^{53}Mn–^{53}Cr system of HED meteorites indicates that the fractionation process in the HED parent body mantle took place within a few million years after CAIs (Lugmair and Shukolyukov, 1998). Those evidence indicate that the meteorite parent bodies formed even earlier than 3 My after CAIs, so that the chondrule formation was simultaneous with planetary formation, if younger ages obtained by Russell et al. (1996; 1997) were the real formation ages of chondrules. This caused Sears (1998) and Hewins et al. (1998) to consider that the ^{26}Al ages as young as 5 My after CAIs are the evidence of chondrule formation through planetary processes. In the present study, the time of chondrule formation was found to be nearly 2 My after CAIs, which does not reach 5 My after CAIs when planetary processes undoubtedly had started. Although it is possible that the earliest planetary process started as early as 2 My after CAIs and chondrules formed on the pre-existing parent bodies, there is no direct evidence for the planetary process occurred at 2 My after CAIs. For this reason, our results rather support the remelting model in the solar nebula.

Absence of chondrules with ages much older than 2 My indicates that chondrule formation did not start for ~2 My after CAIs formation. There are few examples of CAIs inside ferromagnesian chondrules, but no chondrule is included in CAIs (McSween, 1977), which is consistent with the results of ^{26}Al chronology of CAIs and chondrules. Five chondrules studied here show various chemical composition and petrologic texture, indicating that they represent majority of chondrules in Semarkona.

Alternatively, the older records of chondrule formation were overprinted by those of the last heating processes. Presence of relict grains in many chondrules (Nagahara, 1981; Jones, 1996b) is interpreted to represent the formation of chondrules by remelting of earlier generation of chondrules. If many chondrules experienced the final remelting at nearly 2 My, it may be difficult to find chondrules with old ages even though the chondrule formation started much earlier than 2 My. During this process, it is possible that old CAIs might be consumed, resulted in low abundance of CAIs in ordinary chondrites (~10% for CO and CV and less than 1% for ordinary chondrites). For this reason, though our results suggest the short duration of chondrule formation, we need much more data including chondrules from other chondrite groups to clarify if there is any chondrules with older ages or not.

Finally, the obtained formation time relative to CAIs is based on the assumption that the ^{26}Al was homogeneously distributed in the early solar system. However, there is a possibility that the initial relative abundance of ^{26}Al in CAIs was significantly higher than that of ordinary chondrites. Then, the direct chronological use of the ^{26}Al/^{27}Al ratios in CAIs and ferromagnesian chondrules is not justified. The assumption on the ^{26}Al isotopic homogeneity should be tested by the multiple dating systems. However, at the present, it is very difficult to detect the formation time interval of 2 My between CAIs and chondrules by other dating methods. An application of the ^{53}Mn–^{53}Cr and ^{60}Fe–^{60}Ni systems for studies of CAIs has serious difficulties because of the presence of pre-solar Cr and Ni components that may obscure the observation of the radiogenic

isotopes (Shukolyukov and Lugmair, 1993a; Lugmair and Shukolyukov, 1988). The I–Xe system in the CAIs seems to be affected by secondary processes in parent bodies (Swindle et al., 1988). The U–Pb dating of chondrules is technically difficult because of low U contents. The recent finding of former presence of live ^{41}Ca in the solar system (Srinivasan et al., 1994) suggests that the comparison of the ^{26}Al–^{26}Mg and ^{41}Ca–^{41}K systems may clarify the problem of the isotopic heterogeneity of the short lived nuclides. However, the half-life of ^{41}Ca is only 0.1 My, which is too short to examine the time difference in the range of several millions of years.

4. CONCLUSIONS

The following conclusions were obtained from the SIMS ^{26}Al–^{26}Mg and ^{60}Fe–^{60}Ni analyses of the ferromagnesian chondrules from the least equilibrated ordinary chondrite Semarkona (LL3.0).

(1) The study of high Al/Mg glass and plagioclase in common chondrules has revealed the presence of excesses radiogenic ^{26}Mg. Two chondrules show well-defined ^{26}Al–^{26}Mg isochrons, which is the first evidence of former presence of the live-^{26}Al in type II chondrules.

(2) The estimated ^{26}Al/^{27}Al ratios at the time of chondrule formation are between 6×10^{-6} and 9×10^{-6}. The values obtained from various types of chondrules agree within the uncertainties, indicating that various types of chondrules formed within a short duration of time less than 1 My. Assuming the homogeneous distribution of Al isotopes in the early solar system, chondrule formation occurred 2 My after CAI formation. If chondrule formation started earlier, absence of older chondrules indicates that the old records were erased by the chondrule recycling process.

(3) The initial ^{26}Al/^{27}Al ratios of Semarkona chondrules are higher than those of many Al-rich chondrules in UOCs with higher petrologic subtype (Russell et al., 1996; 1997), suggesting that the latter younger ^{26}Al ages would be apparent due to disturbance during the parent body metamorphism. The present results are not in agreement with the previous work that indicated the extended nebular time scale of >5 My and chondrule formation by the planetary processes.

(4) The Ni isotopic analyses of olivines in a type II chondrule in Semarkona do not show any detectable ^{60}Ni excess. The upper limit of ^{60}Fe/^{56}Fe ratio of the initial solar system is estimated to be 3.4×10^{-7}, which is significantly lower than the earlier estimate derived from CAIs, but agrees with the estimate of $(0.2–1.9) \times 10^{-7}$ from eucrite samples (Shukolyukov and Lugmair, 1996).

For future ^{26}Al–^{26}Mg studies on chondrule formation processes, its relationship to the CAI formation, and life time of the solar nebula, detailed studies on a variety of chondrules should focus on samples from the least metamorphosed chondrites like Semarkona.

MS analyses of plagioclase standards, K. Tsukimura for preparing glass standards, and I. Miyagi for the use of his glass standard.

REFERENCES

Alexander C. M. O'D., Barber D. J., and Hutchison R. (1989) The microstructure of Semarkona and Bishunpur. *Geochim. Cosmochim. Acta* **53,** 3045–3057.

Allen J. M., Grossman L., Davis A. M., and Hutcheon I. D. (1978) Mineralogy, textures and mode of formation of a hibonite-bearing Allende inclusion. Proceedings of the 9th Lunar and Planetary Science Conference, pp. 1209–1233.

Birck J. L. and Lugmair G. W. (1988) Nickel and chromium isotopes in Allende inclusions. *Earth Planet. Sci. Lett.* **90,** 131–143.

Catanzaro E. J., Murphy T. J., Garner E. L., and Shields W. R. (1966) Absolute isotopic abundance ratios and atomic weights of magnesium. *J. Res. Natl. Bur. Stand.* **70a,** 453–458.

Ebel D. S. and Grossman L. (2000) Condensation in dust-enriched systems. *Geochim. Cosmochim. Acta* **64,** 339–366.

Fuchs L. H. (1971) Occurrence of wollastonite, rhönite, and andradite in the Allende meteorite. *Amer. Mineral.* **56,** 2053–2068.

Göpel C., Manhès G., and Allègre C. J. (1994) U–Pb systematics of phosphates from equilibrated ordinary chondrites. *Earth Planet. Sci. Lett.* **121,** 153–171.

Grossman J. N., Alexander C. M. O'D., Wang J., and Brearley A. J. (2000) Bleached chondrules: Evidence for widespread aqueous processes on the parent asteroids of ordinary chondrites. *Meteorit. Planet. Sci.* **35,** 467–486.

Hewins R. H., Zanda B., Yang Y., and Bourot-Denise M. (1998) Towards a new model for chondrules. *Paul Pellas Symposium*, pp. 31–34. Museum National d'Histoire Naturelle.

Hutcheon I. D. and Hutchison R. (1989) Evidence from the Semarkona ordinary chondrite for [26]Al heating of small planets. *Nature* **337,** 238–241.

Hutcheon I. D. and Jones R. H. (1995) The [26]Al–[26]Mg record of chondrules: Clues to nebular chronology. *Lunar Planet. Sci.* **26,** 647–648.

Hutcheon I. D., Huss G. R., and Wasserburg G. J. (1994) A search for [26]Al in chondrites: Chondrule formation time scales. *Lunar Planet. Sci.* **25,** 587–588.

Jones R. H. (1990) Petrology and mineralogy of type II, FeO-rich chondrules in Semarkona (LL3.0): Origin by closed-system fractional crystallization, with evidence for supercooling. *Geochim. Cosmochim. Acta* **54,** 1785–1802.

Jones R. H. (1994) Petrology of FeO-poor, porphyritic pyroxene chondrules in the Semarkona chondrite. *Geochim. Cosmochim. Acta* **58,** 5325–5340.

Jones R. H. (1996a) FeO-rich, porphyritic pyroxene chondrules in unequilibrated ordinary chondrites. *Geochim. Cosmochim. Acta* **60,** 3115–3138.

Jones R. H. (1996b) Relict grains in chondrules: Evidence for chondrule recycling. In *Chondrules and the Protoplanetary Disk* (eds. R. H. Hewins et al.), pp. 163–172. Cambridge University Press.

Jones R. H. and Scott E. R. D. (1989) Petrology and thermal history of type IA chondrules in the Semarkona (LL3.0) chondrite. Proceedings of the 19th Lunar and Planetary Science Conference, pp. 523–536.

Kita N. T., Togashi S., Morishita Y., Terashima S., and Yurimoto H. (1998) Search for [60]Ni excesses in MET-78008 ureilite: An microprobe study. *Antarct. Meteorite Res.* **11,** 103–121.

LaTourrette T. and Wasserburg G. J. (1998) Mg diffusion in anorthite: Implications for the formation of early solar system planetesimals. *Earth Planet. Sci. Lett.* **158,** 91–108.

Ludwig K. R. (1989) ISOPLOT: A plotting and regression program for radiogenic-isotope data; USGS Open-File Report 91.

Lugmair G. W. and Shukolyukov A. (1998) Early solar system timescales according to [53]Mn–[53]Cr systematics. *Geochim. Cosmochim. Acta* **62,** 2863–2886.

MacPherson G. J., Davis A. M., and Zinner E. K. (1995) The distribution of aluminum-26 in the early Solar System—A reappraisal. *Meteoritics* **30,** 365–386.

McCoy T. J., Scott E. R. D., Jones R. H., Keil K., and Taylor G. J. (1991) Composition of chondrule silicates in LL3–5 chondrites and implications for their nebular history and parent body metamorphism. *Geochim. Cosmochim. Acta* **55,** 601–619.

McSween H. Y. (1977) Chemical and petrographic constraints on the origin of chondrules and inclusions in carbonaceous chondrites. *Geochim. Cosmochim. Acta* **41,** 1843–1860.

Morishita Y., Sasaki A., Kita N. T., and Togashi S. (1998) Microanalysis for sulfur and oxygen isotopic ratios using SIMS. In *Secondary Ion Mass Spectrometry SIMS XI* (eds. G. Gillen et al.), pp. 67–70.

Nagahara H. (1981) Evidence for secondary origin of chondrules. *Nature* **292,** 135–136.

Nyquist L. E., Lindstrom D., Shih C.-Y., Wiesmann H., Mittlefehldt D., Wentworth S., and Martinez R. (1997) Mn–Cr isotopic systematics of chondrules from the Bishunpur and Chainpur meteorites. *Lunar Planet. Sci.* **28,** 1093–1094.

Nyquist L. E., Shih C.-Y., Wiesmann H., Reese Y., Ulyanov A. A., and Takeda H. (1999) Towards a Mn–Cr timescale for the early solar system. *Lunar Planet. Sci.* **30,** Abstract #1604, Lunar and Planetary Institute, Houston (CD-ROM).

Russell S. S., Srinivasan G., Huss G. R., Wasserburg G. J., and MacPherson G. J. (1996) Evidence for widespread [26]Al in the solar nebula and constraints for nebula time scales. *Science* **273,** 757–762.

Russell S. S., Huss G. R., MacPherson G. J., and Wasserburg G. J. (1997) Early and late chondrule formation: New constraints for solar nebula chronology from [26]Al/[27]Al in unequilibrated ordinary chondrites. *Lunar Planet. Sci.* **28,** 1209–1210.

Scott E. R. D. and Taylor G. J. (1983) Chondrules and other components in C, O, and E chondrites: Similarities in their properties and origins. Proceedings of the 14th Lunar and Planetary Science Conference. *J. Geophys. Res.* **88,** Suppl. B275–B286.

Sears D. W. G. (1998) The origin of chondrules and chondrites. *Papers Presented to the Twentythird Symposium on Antarctic Meteorites*, pp. 134–138. National Institute of Polar Research.

Sears D. W., Grossman J. N., Melcher C. L., Ross L. M., and Mills A. A. (1980) Measuring metamorphic history of unequilibrated ordinary chondrites. *Nature* **287,** 791–795.

Sears D. W. G., Hasan F. A., Batchelor J. D., and Lu J. (1991) Chemical and physical studies of type 3 chondrites-XI: Metamorphism, paring, and brecciation of ordinary chondrites. Proceedings of the 21st Lunar and Planetary Science Conference, pp. 493–512.

Sears D. W. G., Jie L., Benoit P. H., DeHart J. M., and Lofgren G. E. (1992) A compositional classification scheme for meteoritic chondrules. *Nature* **357,** 207–210.

Shukolyukov A. and Lugmair G. W. (1993a) Live Iron-60 in the early solar system. *Science* **259,** 1138–1142.

Shukolyukov A. and Lugmair G. W. (1993b) [60]Fe in eucrites. *Earth Planet. Sci. Lett.* **119,** 159–166.

Shukolyukov A. and Lugmair G. W. (1996) Iron-60/Nickel-60 isotope system in the eucrite Caldera. *Meteoritics* **31,** A129.

Srinivasan G., Ulyanov A. A., and Goswami J. N. (1994) [41]Ca in the early solar system. *Astrophys. J.* **431,** L67–L70.

Srinivasan G., Russell S. S., MacPherson G. J., Huss G. R., and Wasserburg G. J. (1996) New evidence for [26]Al in CAI and chondrules from type 3 ordinary chondrites. *Lunar Planet. Sci.* **27,** 1257–1258.

Stoll B. and Jochum K. P. (1999) MIC-SSMS analyses of eight new geological standard glasses. *Fresenius J. Anal. Chem.* **364,** 380–384.

Swindle T. D., Caffee M. W., and Hohenberg C. M. (1988) Iondine-Xenon studies of Allende inclusions: Eggs and the Pink Angel. *Geochim. Cosmochim. Acta* **52,** 2215–2227.

Wark D. A. and Lovering J. F. (1977) Marker events in the early evolution of the solar system: Evidence from rims on Ca–Al-rich inclusions in carbonaceous chondrites. Proceedings of the 8th Lunar and Planetary Science Conference, pp. 95–112.

Wasserburg, G. J., Busso M., Gallino R., and Raiteri C. M. (1994) Asymptotic giant branch stars as a source of short-lived radioactive nuclei in the solar nebula. *Astrophys. J.* **424,** 412–428.

Wasserburg G. J., Gallino R., and Busso M. (1998) A test of the supernova trigger hypothesis with [60]Fe and [26]Al. *Astrophys. J.* **500,** L189–L193.

Wood, J. A. (1962) Chondrules and the origin of the terrestrial planets. *Nature* **197,** 127–130.

Yoneda S. and Grossman L. (1995) Condensation of CaO–MgO–Al_2O_3–SiO_2 liquids from cosmic gases. *Geochim. Cosmochim. Acta* **59,** 3413–3444.

Zinner E. and Göpel C. (1992) Evidence for [26]Al in feldspars from the H4 chondrite Ste. Marguerite. *Meteoritics* **27,** 311–312.